Noise-Induced Roughening Evolution of Amorphous Si films Grown by Thermal Evaporation

H.-N. Yang, Y.-P. Zhao, G.-C. Wang, and T.-M. Lu

Department of Physics, Applied Physics, and Astronomy, and Center for Integrated Electronics and Electronics Manufacturing, Rensselaer Polytechnic Institute, Troy, New York 12180-3590

(Received 4 December 1995)

We report a growth front morphology study of thermally evaporated amorphous Si films using atomic force microscopy. Since there are no well-defined atomic steps on an amorphous film surface, there is no Schwoebel barrier effect which would give rise to a moundlike morphology. The dynamic scaling characteristics observed during growth are unambiguously explained by a noise-induced growth mechanism. The roughness and growth exponents measured are consistent with the Mullins diffusion model with noise. [S0031-9007(96)00135-4]

PACS numbers: 68.55.Jk, 64.60.Ht, 68.35.Bs

Interface roughness is one of the central features in many important thin film technologies, since it directly controls many physical and chemical film properties. Reduction of roughness is desirable in many thin film applications, particularly for many quantum well multilayer structures. But, for many other applications, rough interfaces can be very useful, e.g., catalysis and adhesion enhancement between materials. Roughness can be created during growth or etching of the film surface. Recently, intense effort has been put into the study of the origin of the formation of rough surfaces during growth or etching [1–5]. There have been two major mechanisms proposed. One mechanism is based on noise-induced roughening which gives rise to the very interesting phenomenon of dynamic scaling [6]. The other mechanism has to do with the existence of a diffusion barrier (Schwoebel barrier [7]) at a step edge which prevents an atom from jumping downward to a terrace, and therefore would generate a rough surface containing mounds [8]. In the last few years, the validity of the theory based on the noise-induced roughening has faced serious challenges from experimental observations on molecular beam epitaxy (MBE) [1(c),9]. Tremendous debate, controversy, and confusion have been generated regarding which mechanism plays a more important role in thin film growth. The situation is worse when both mechanisms may exist in a single experiment [10].

The Schwoebel barrier effect is unlikely to play an important role in amorphous film growth because of the lack of well-defined atomic steps at the surface. The study of amorphous film growth may therefore allow one to test unambiguously the validity of theories based on the noise-induced growth front roughening. Although some work on the measurement of amorphous growth front roughening has been reported [11–13], a complete understanding of the phenomenon based on recent understanding of dynamic scaling theories has not been established. In this paper, we report a morphology study on the growth of thermally evaporated amorphous Si films using atomic force microscopy (AFM). We found that the amorphous Si films did not have moundlike morphology. With a low substrate temperature of <300 K, the growth front evolution of the amorphous Si film demonstrated rich dynamic scaling characteristics. Detailed analysis indicated that the Si amorphous growth can be explained by the noise-driven, Mullins diffusion mechanism.

The amorphous Si films were grown by thermal evaporation of 99.999% pure Si source onto Si substrates at normal incidence in a high vacuum chamber (base pressure $\sim 2 \times 10^{-6}$ torr). The evaporator consists of a graphite boat in which the Si source is placed. Evaporation is achieved by electron bombardment of the Si source using a heated Ta filament. This design can provide a stable deposition rate. The deposition rate was 0.8 ± 0.2 Å/sec. The Si wafers had a (111) orientation and were cleaned using a dilute Hartree-Fock (HF) dip [1:10(49%HF:H_2O)] before being placed in the chamber. The Si substrate was maintained at 11 °C through the contact with a Cu cold finger which was cooled by chilled water during deposition. The films were amorphous under this deposition condition. The samples were deposited for different deposition times ranging from a few minutes to more than 10 h. For each Si film, the deposition always started with a fresh Si wafer and then proceeded continuously without interruption to the targeted time. After deposition, each Si wafer was taken out for immediate *ex situ* AFM measurements. The AFM scans were carried out using a Park Scientific Instruments AutoProbe CP with a Si_3N_4 tip. The typical radius and side angle of the tips are about 100 Å and 10°, respectively. Such a tip allows us to measure reliably the scale of the surface roughness profile presented in this work according to the criterion set by Griffith and Grigg [14].

AFM images of 512×512 data points were obtained with scanning areas ranging from 0.1×0.1 up to 5×5 μm^2. Figure 1 shows some 1×1 μm^2 surface images of the amorphous Si films deposited for $t = 0.25$, 0.75, 1.5, 3, 5, and 8 h. The 1D cross section scans of surface profiles are also plotted in Fig. 2 for $t = 3$, 5, and 8 h. Two typical morphological features can be recognized readily by visual inspection of Figs. 1

 0031-9007/96/76(20)/3774(4)$10.00 © 1996 The American Physical Society

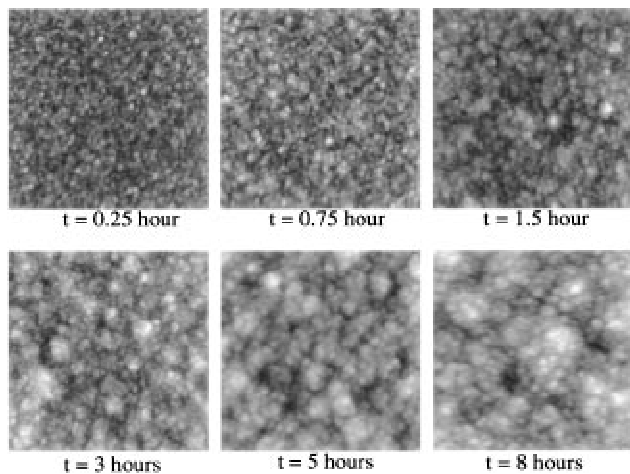

FIG. 1. AFM images ($1 \times 1\ \mu m^2$) of amorphous Si films deposited at room temperature for $t = 0.25$, 0.75, 1.5, 3, 5, and 8 h.

and 2. The first feature is that the random roughness of various scales exists in all the films. For example, the mountains and valleys as well as island clusters, as shown in films at 1.5, 3, 5, and 8 h, possess different sizes and separations, and irregular shapes. The second characteristic of these films is the evolution of the surface roughness as a function of deposition time, where mountains, valleys, and island clusters are becoming bigger and bigger as films grow thicker.

The morphology of the amorphous films shown in Figs. 1 and 2 is distinctly different from that of a crystalline film grown under the influence of a Schwoebel barrier. In the presence of a diffusion barrier, the growing morphology exhibits a moundlike structure having a fairly regular shape, stable local slope (slope selection), and well-defined size and separation (wavelength selection) [8,15,16]. Such regularities have been observed in several MBE grown films. Examples are GaAs/GaAs(001) [17], Ge/Ge(001) [18], and Fe/Fe(001) [19,20]. These regularities are not seen for our amorphous Si films. To quantitatively examine the characteristics of the morphology, we plot in Fig. 3 the autocorrelation function, $\langle [h(\boldsymbol{r},t)h(0,t)] \rangle$ as a function of position $\boldsymbol{r}$ for different films. $\boldsymbol{r}$ denotes the lateral surface position, and $h(\boldsymbol{r},t)$ is the relative surface height at position $\boldsymbol{r}$ and deposition time t with respect to the average surface height $\langle h(t) \rangle$ or the film thickness. In order to obtain a good statistical average, we calculated the correlation function by averaging over at least ten images measured at different regions in each film. A total of 512 line scans were obtained for each image. No clear oscillatory behavior is seen in the autocorrelation plot. This is an indication of the lack of wavelength selection which should exist if a Schwoebel barrier plays an important role. We shall also show later that there is no surface slope selection in this system.

In Fig. 4, we plot the height-height correlation functions, $H(\boldsymbol{r},t) = \langle [h(\boldsymbol{r},t) - h(0,t)]^2 \rangle$, as a function of position $\boldsymbol{r}$ for different values of t or film thickness. The dynamic scaling hypothesis suggests that the height-height correlation has the scaling form

$$H(\boldsymbol{r},t) \sim \begin{cases} Cr^{2\alpha} & \text{for } r \ll \xi(t), \\ 2w^2(t) & \text{for } r \gg \xi(t), \end{cases} \tag{1}$$

where α is called the roughness exponent and which describes how "wiggly" the local slope is. $\xi(t)$ is the lateral correlation length which is defined as the largest distance in which the height is still correlated. $w = \{\langle [h(\boldsymbol{r},t)]^2 \rangle\}^{1/2}$ is the interface width which is a measure

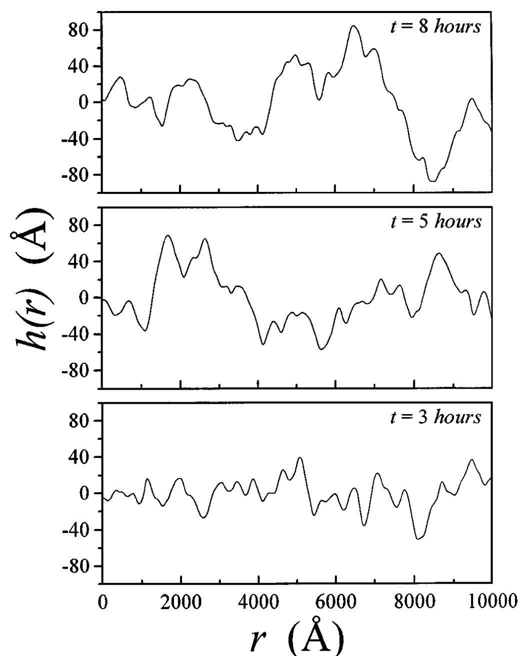

FIG. 2. 1D AFM surface profile scans of amorphous Si films are plotted for $t = 3$, 5, and 8 h. $h(r)$ is the height of the surface at position r.

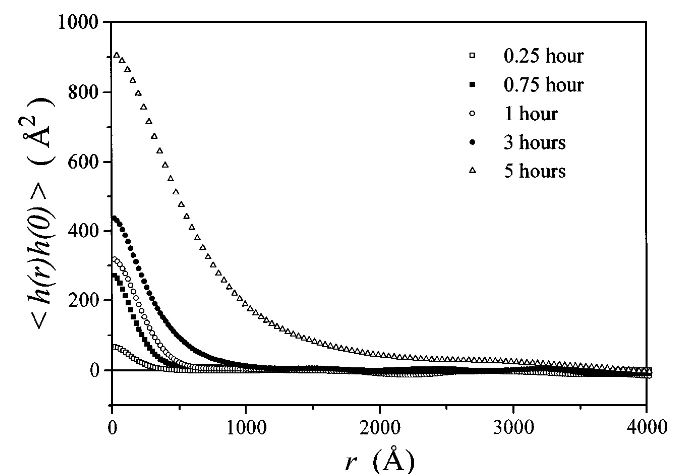

FIG. 3. The autocorrelation function, $\langle [h(\boldsymbol{r},t)h(0,t)] \rangle$, is plotted as a function of position r for different deposition time.

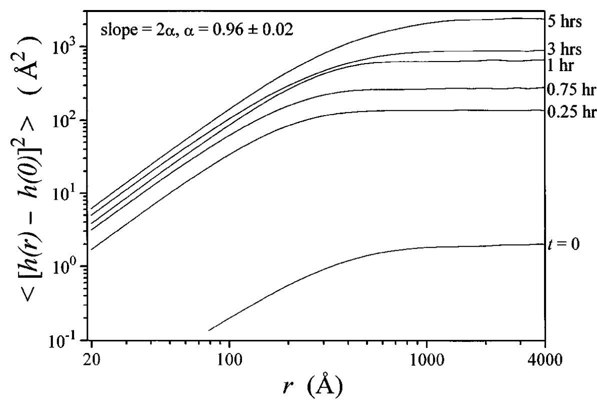

FIG. 4. The height-height correlation functions, $H(\boldsymbol{r}, t) = \langle [h(\boldsymbol{r}, t) - h(0, t)]^2 \rangle$, is plotted as a function of the position r for different deposition time. The slope of the curves for small r gives 2α, where α is the roughness exponent. The intersection of the curves with the vertical axis is related to the local surface slope of the films.

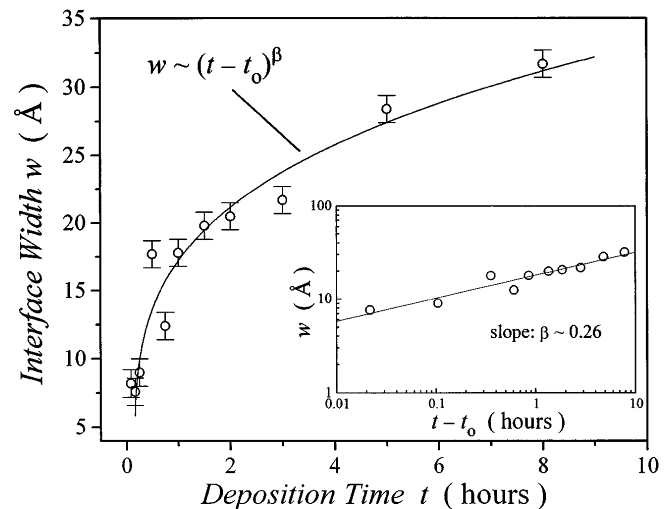

FIG. 5. The interface width w of each film for different deposition time is plotted as a function of t. The solid curve is a fit with the functional form $w \propto (t - t_0)^\beta$. The fit gives $\beta \approx 0.26 \pm 0.02$ and $t_0 = 0.13 \pm 0.01$ h. Shown in the inset is a log-log plot of w as a function of $t - t_0$.

of the surface height fluctuation, and is proportional to t^β where β is the growth exponent. Note that ξ provides a length scale which distinguishes the short-range and long-range behaviors of the rough surface. Equation (1) suggests that the morphology of the growing interface has both a short-range spatial scaling and a long-range time scaling.

Both the short-range spatial scaling and long-range roughening evolution are demonstrated clearly in the log-log plots of $H(\boldsymbol{r}, t)$ vs r shown in Fig. 4 for the present amorphous Si experimental data. $H(\boldsymbol{r}, t)$ varies with r in the form of a power law for small r. The slope of the plots is about the same for all t (or for all thickness of the films) and gives $\alpha = 0.96 \pm 0.02$. At sufficiently large r, each curve turns into a plateau. The turning point determines the lateral correlation $\xi(t)$, and the plateau depends on the interface width w with $H(\boldsymbol{r}, t) \approx 2w^2$. We measured the interface width w of each film for different deposition time and then plotted w as a function of t in Fig. 5. We fit the data using the form $w \propto (t - t_0)^\beta$, where β and t_0 are adjustable parameters. t_0 is a small number and is a measure of the initial transient growth time where the dynamic scaling has not occurred. The result of the fit is shown as the solid curve in Fig. 5 and gives $\beta \approx 0.26 \pm 0.02$ and $t_0 = 0.13 \pm 0.01$ h. To demonstrate the power-law relationship more clearly, we also replot w against $t - t_0$ in the log-log plot as shown in the inset of Fig. 5.

There are two different types of dynamic scaling behavior in growth front roughening. The first type has a self-affine and time-invariant growth morphology on the short-range scale characterized by a roughness exponent $0 \leq \alpha < 1$ and a time-independent coefficient C [1,6]. In this case, the fluctuations and the smoothing effect at the growth front reach a balance, and the local structure remains unchanged. The local surface slope has been shown to be proportional to $\sqrt{C}$ [21]. The second type of dynamic scaling is called anomalous dynamic scaling which gives $\alpha \geq 1$, and the value of C increases with time [22–25]. Obviously, this is a situation where the fluctuations and the smoothing effect cannot quite reach a balance, and the local surface slope keeps growing with time. From Fig. 4, it is seen that our amorphous Si growth belongs to the second type, where the local slope changes with time and has an α value close to 1.

Our amorphous Si growth behavior is, in fact, quite consistent with the noise-driven Mullins diffusion model [22–24]. In this model, the surface diffusion is driven by the gradient of local surface curvature and can be represented approximately by a gradient term, $-\nabla^4 h$. Combining this smoothing mechanism with random fluctuations that exist during deposition, one can describe the growth process by a Langevin equation of the form $\partial h(\boldsymbol{r}, t)/\partial t = -\nabla^4 h(\boldsymbol{r}, t) + \eta$, where η is white noise simulating random fluctuations during growth. This equation can be solved analytically giving a height-height correlation function in the form of Eq. (1), with $\alpha = 1$, $\beta = 0.25$, and a time dependent C. It appears that both short-range and long-range behaviors observed in the present experiment can be described quite well by this model.

It is of interest to note that dynamic scaling may also occur in epitaxial growth or etch fronts of Si/Si [26–28] at above room temperature. In particular, electron diffraction study of the epitaxial growth of Si on Si(111) [27] and sputtered etching of Si(111) surface [28] indicated that the Mullins diffusion mechanism played an important role in the roughening evolution of the growth or etch fronts. However, it has also been shown that, depending on the surface preparation, faceting (similar to the mound

formation) can also occur in epitaxial growth of Si/Si(111) [29]. More study is needed to quantify the Schwoebel barrier height and to clarify the role of an asymmetric diffusion barrier in the epitaxial growth and etch fronts of crystalline Si surfaces. In any case, our present amorphous Si growth clearly indicates the existence of a random noise during deposition and the importance of noise-induced roughening of a growth front in the absence of a Schwoebel barrier.

This work is supported by NSF DMR-9213023. We thank G.-R. Yang for his help in the evaporation and Steve Soss for his help in taking the AFM images. We also thank Dr. J. Amar, Dr. K. S. Liang, and Dr. D. Y. Noh for valuable discussions.

[1] *Dynamics of Fractal Surfaces,* edited by F. Family and T. Vicsek (World Scientific, Singapore, 1991); Tamas Vicsek, *Fractal Growth Phenomena* (World Scientific, Singapore, 1992); *Fractal Aspects of Materials,* edited by F. Family, P. Meakin, B. Sapoval, and R. Wool, MRS Symposia Proceedings No. 367 (Materials Research Society, Pittsburgh, 1995).

[2] J. Krug and H. Spohn, in *Solids Far from Equilibrium,* edited by C. Godreche (Cambridge University Press, Cambridge, England, 1991); *Surface Disordering: Growth, Roughening, and Phase Transition,* edited by R. Jullien, J. Kertesz, P. Meakin, and D. E. Wolf (Nova Science Publishers, Inc., Commack, 1992); *Scale Invariance, Interfaces, and Nonequilibrium Dynamics,* edited by Alan McKane, Michel Droz, Jean Vannimenus, and Dietrich Wolf, NATO ASI Series B, Vol. 344 (Plenum Press, New York, 1995).

[3] H.-N. Yang, G.-C. Wang, and T.-M. Lu, *Diffraction from Rough Surfaces and Dynamic Growth Fronts* (World Scientific, Singapore, 1993).

[4] A.-L. Barabasi and H. E. Stanley, *Fractal Concepts in Surface Growth* (Cambridge University Press, Cambridge, England, 1995).

[5] J. Krim and G. Palasantzas, Int. J. Mod. Phys. B **9**, 599 (1995); J. Lapujoulade, Surf. Sci. Rep. **20**, 191 (1994); P. Meakin, Phys. Rep. **235**, 189 (1993).

[6] F. Family and T. Vicsek, J. Phys. A **18**, L75 (1985); F. Family, Physica (Amsterdam) **168A**, 561 (1990).

[7] R. L. Schwoebel and E. J. Shipsey, Appl. Phys. **37**, 3682 (1966); R. L. Schwoebel, J. Appl. Phys. **40**, 614 (1968).

[8] J. Villain, J. Phys. (France) I **1**, 19 (1991).

[9] For a review, see *Fractal Concepts in Surface Growth* (Ref. [4]), Chap. 16.

[10] For example, K. Fang, T.-M. Lu, and G.-C. Wang, Phys. Rev. B **49**, 8331 (1994).

[11] D. J. Eaglesham and G. H. Gilmer, in *Surface Disordering: Growth, Roughening, and Phase Transition* (Ref. [2]), p. 69.

[12] T. Yoshinobu, A. Iwamoto, K. Sudoh, and H. Iwasaki, in *Fractal Aspects of Materials* (Ref. [1]), p. 329.

[13] D. M. Tanenbaum, A. Laracuente, and A. C. Callagher, in *Amorphous Silicon Technology-1994,* edited by E. A. Schiff, M. Hack, A. Madan, M. Powell, and A. Matsuda, MRS Symposia Proceedings No. 336 (Materials Research Society, Pittsburgh, 1994).

[14] J. E. Griffith and D. A. Grigg, J. Appl. Phys. **74**, R83 (1993).

[15] A. W. Hunt, C. Orme, D. R. M. Williams, B. G. Orr, and L. M. Sander, Europhys. Lett. **27**, 611 (1994).

[16] M. Siegert and M. Plischke, Phys. Rev. Lett. **73**, 1517 (1994).

[17] M. D. Johnson, C. Orme, A. W. Hunt, D. Graff, J. Sudijono, L. M. Sander, and B. G. Orr, Phys. Rev. Lett. **72**, 116 (1994).

[18] J. E. Van Nostrand, S. J. Chey, M.-A. Hasan, D. G. Cahill, and J. E. Greene, Phys. Rev. Lett. **74**, 1127 (1995).

[19] J. A. Stroscio, D. T. Pierce, M. Stiles, A. Zangwill, and L. M. Sander, Phys. Rev. Lett. **75**, 4246 (1995).

[20] K. Thurmer, R. Koch, M. Weber, and K. H. Rieder, Phys. Rev. Lett. **75**, 1767 (1995).

[21] H.-N. Yang, G.-C. Wang, and T.-M. Lu, Phys. Rev. Lett. **74**, 2276 (1995).

[22] D. E. Wolf and J. Villain, Europhys. Lett. **13**, 389 (1990).

[23] S. Das Sarma and P. I. Tamborenea, Phys. Rev. Lett. **66**, 325 (1991).

[24] J. G. Amar, P.-M. Lam, and F. Family, Phys. Rev. E **47**, 3242 (1993).

[25] For a review, see T.-M. Lu, H.-N. Yang, and G.-C. Wang, in *Fractal Aspects of Materials* (Ref. [1]), p. 283.

[26] P. E. Hegeman, H. J. W. Zandvliet, G. A. M. Kip, and A. Van Silfhout, Surf. Sci. **311**, L655 (1994).

[27] H.-N. Yang, G.-C. Wang, and T.-M. Lu, Phys. Rev. Lett. **73**, 2348 (1994).

[28] H.-N. Yang, G.-C. Wang, and T.-M. Lu, Phys. Rev. B **50**, 7635 (1994).

[29] N.-N. Yang, G.-C. Wang, and T.-M. Lu, Phys. Rev. B **51**, 14 293 (1995).